



Article

Behavior of Glass-like and Mineral-like Phosphate Compounds with an Immobilized Chloride Mixture in Hydrogen Peroxide Solutions

Anna V. Frolova , Svetlana A. Kulikova , Kseniya Y. Belova, Sergey S. Danilov and Sergey E. Vinokurov *

Vernadsky Institute of Geochemistry and Analytical Chemistry of Russian Academy of Sciences, 19 Kosygin st., 119991 Moscow, Russia

* Correspondence: annav1805@gmail.com (A.V.F.); vinokurov.geokhi@gmail.com (S.E.V.);
Tel.: +7-495-939-7007 (A.V.F.)

Abstract: A new type of high-level waste (HLW) is generated during pyrochemical reprocessing of mixed nitride spent uranium–plutonium nuclear fuel. Such waste is a spent electrolyte, which is a mixture of chloride salts containing approximately 25.7 wt.% LiCl + 31.6 wt.% KCl + 4.1 wt.% CsCl + 5.1 wt.% BaCl₂ + 3.8 wt.% SrCl₂ + 29.7 wt.% LaCl₃, and its immobilization in reliable matrices is an actual radiochemical problem. The structure and hydrolytic stability of sodium aluminophosphate (NAFP) glass and a low-temperature mineral-like magnesium potassium phosphate (MPP) matrix, which are promising for spent electrolyte immobilization in the presence of hydrogen peroxide solutions simulating natural water radiolysis products, were studied in this work. The structure of the samples was studied using the SEM-EDS method. It was shown that the initial samples of NAFP glass after leaching in hydrogen peroxide solutions are prone to precipitation of crystalline phases on the surface, which are mainly represented by a mixture of sodium–iron–aluminum pyrophosphates. It was established that the leaching rate of structure-forming components of NAFP and MPP matrices generally increase, but remain at a low level, meeting modern requirements for HLW immobilization. This confirms the effectiveness of the studied matrices for the industrial use of the spent electrolyte.

Keywords: sodium aluminophosphate glass; magnesium potassium phosphate compound; radioactive waste; spent electrolyte; chlorides; immobilization; leaching; hydrogen peroxide; thermal stability; structure



Citation: Frolova, A.V.; Kulikova, S.A.; Belova, K.Y.; Danilov, S.S.; Vinokurov, S.E. Behavior of Glass-like and Mineral-like Phosphate Compounds with an Immobilized Chloride Mixture in Hydrogen Peroxide Solutions. *Energies* **2022**, *15*, 6477. <https://doi.org/10.3390/en15176477>

Academic Editor: Jong-Il Yun

Received: 1 August 2022

Accepted: 2 September 2022

Published: 5 September 2022

Publisher's Note: MDPI stays neutral with regard to jurisdictional claims in published maps and institutional affiliations.



Copyright: © 2022 by the authors. Licensee MDPI, Basel, Switzerland. This article is an open access article distributed under the terms and conditions of the Creative Commons Attribution (CC BY) license (<https://creativecommons.org/licenses/by/4.0/>).

1. Introduction

To date, the management of high-level waste (HLW) involves conditioning and disposal in deep geological formations. It is supposed that a multi-barrier concept is implemented, where the first barrier is a preservative matrix [1]. Borosilicate or aluminophosphate glass is used as such matrix for HLW immobilization [2]. Recently, much attention has been paid to the modernization of existing glass matrices and the search for new types of matrix materials. Various ceramic and glass–ceramic matrices have been considered [3,4].

At the same time, with the development of nuclear energy, more and more accumulated radioactive waste is appearing that is not suitable for immobilization in high-temperature glass (the temperature of phosphate glass synthesis is 900–1050 °C [5]; for borosilicate glass, it is about 1150 °C [6]). Thus, a new type of waste, spent electrolyte, which is a mixture of alkali metal chlorides in the LiCl–KCl–NaCl–CsCl system containing actinide residues and fission products, primarily cesium isotopes volatilized at high temperatures, is formed during the pyrochemical processing of mixed uranium–plutonium nitride spent nuclear fuel (MNUP SNF) of the BREST-OD-300 reactor plant with a lead coolant [7]. The incorporation of chlorides into glasses is also prevented by their low solubility in glasses, e.g., less than 1.5% in borosilicate glass [8].

Currently, a search is underway for alternative matrix materials for the immobilization of HLW-containing chlorides. Previously [9], we considered matrices that are promising for the immobilization of spent electrolyte: sodium aluminosilicophosphate (NAFP) glass, which has a lower synthesis temperature compared to aluminophosphate glass [10], as well as mineral-like magnesium potassium phosphate (MPP) compound obtained at room temperature and atmospheric pressure [11]. It was shown that each of the proposed matrices has its own advantages and individual disadvantages in the immobilization of the spent electrolyte. Thus, NAFP glass forms a homogeneous amorphous system and demonstrates low leaching rate of components and high radiation resistance, but can form individual phases on the surface in the form of a thin layer 2–3 μm thick under thermal loads. At the same time, the low-temperature MPP matrix has the advantage of being easy to synthesize, but tends to lose strength under thermal stress. It should be noted that the previous experiments do not allow giving a definite answer about the suitability of NAFP and MPP matrices; thus, further development of studies of these matrices is necessary. Thus, it is known that radiolysis of water occurs under radioactive radiation with the formation of hydrogen peroxide among other products, which will lead to a change in pH and aggressiveness of the leaching medium [12]. The effect of radiolysis products on the leaching rate of components from glass was studied in separate studies [13–15]. The authors of [12] noted that the pH of the leaching solution affects the main leaching mechanisms of glass elements and, as a result, the leaching rate. It is noted that glass corrosion occurs mainly due to the ion exchange in acidic and neutral solutions, but mainly due to the hydrolysis in alkaline solutions. The high rate of the ion exchange in acidic environments at $\text{pH} < 6$ is due to the high concentration of hydronium ions [16]. It was noted in [17] that the negative effect of irradiation begins to be observed already at a low concentration of H_2O_2 and a decrease in pH by 1.

The aim of our work was to study the effect of the presence of H_2O_2 in the leaching solution on the structure of NAFP glass and MPP matrix (as an alternative to high-temperature glass) and on their hydrolytic stability under conditions close to real during radiation of immobilized HLW.

2. Materials and Methods

2.1. Chemicals and Procedures

Different salt electrolyte melts are used as electrolytes under the anhydrous electrochemical processing of MNUP SNF in industry [7]. The spent electrolyte is formed after such processing of SNF, which is contaminated with fission products (primarily Cs, Sr, etc.) and is classified as HLW; hence, it must be converted into stable forms. An imitation of the spent electrolyte with the composition $\text{Li}_{0.4}\text{K}_{0.28}\text{La}_{0.08}\text{Cs}_{0.016}\text{Sr}_{0.016}\text{Ba}_{0.016}\text{Cl}$ (25.7 wt.% LiCl + 31.6 wt.% KCl + 4.1 wt.% CsCl + 5.1 wt.% BaCl₂ + 3.8 wt.% SrCl₂ + 29.7 wt.% LaCl₃) [18] was used to synthesize compounds based on an NAFP glass and MPP matrix. The conditions for the synthesis of the studied compounds are presented below [9].

2.1.1. Synthesis of NAFP Glass

NAFP glass samples of the optimal composition $40\text{Na}_2\text{O}-10\text{Al}_2\text{O}_3-10\text{Fe}_2\text{O}_3-40\text{P}_2\text{O}_5$ (mol.%), which has a high hydrolytic and crystallization stability [19–21], were synthesized with 10 wt.% of the spent electrolyte imitation in the form of dry chloride salts. The samples were synthesized by melting the dry components of the glass batch, namely, $(\text{NH}_4)_2\text{HPO}_4$ (GOST 3772-74), Na_2CO_3 (GOST 4530-76), Al_2O_3 (TU 6-09-426-75), Fe_2O_3 (TU 6-09-5346-87) (Lenreaktiv, St. Petersburg, Russia), and chloride salts, at temperatures up to 1200 °C in quartz crucibles.

The resulting melts were held for 1 h and then poured onto a metal sheet for glass tempering. The calculated elemental composition of the samples (wt.%) is given in Table 1.

Table 1. Calculated elemental composition of NAFP glass samples (wt.%).

Element	Na	P	Fe	Al	Cs	K	Li	La	Sr	Ba	O	Cl
Content	15.4	20.7	9.3	4.5	0.3	1.6	0.4	1.7	0.2	0.3	40.2	5.4

2.1.2. Synthesis of MPP Compound

The samples of low-temperature MPP compound were synthesized at room temperature by mixing the components of MgO:H₂O:KH₂PO₄ matrix at a weight ratio of 1:2:3. For preparing samples, MgO powder (GOST 4526-75, Rushim LLC, Moscow, Russia), initially pre-calcined at 1300 °C for 3 h (specific surface area of 6.6 m²/g), and KH₂PO₄ powder (TU 6-09-5324-87, Chimmed LLC, Moscow, Russia), crushed to a particle size of 0.15–0.25 mm, were used. The spent electrolyte imitation solution, which was obtained by dissolving chloride salts in distilled water (salt content of 554.4 g/L), was solidified. The content of MgO and KH₂PO₄ was calculated on the basis of the water content in the imitation solution. Compounds containing up to 12 wt.% of the spent electrolyte imitation were obtained, as well as synthesized samples containing 23 wt.% of zeolite (hereinafter, these samples are named MPP-Z). The natural zeolite of the Sokyrnytsya deposit, Transcarpathian region (TU 2163-004-61604634-2013, ZEO-MAX LLC, Ramenskoye, Moscow region, Russia), with a particle size of 0.07–0.16 mm and a specific surface area of 17.5 m²/g, was used for increasing the mechanical strength of the MPP compound just as in the previous work [22]. The obtained mixture was placed in a fluoroplastic mold measuring 3 × 1 × 1 cm and left for at least 14 days to set the strength of the compound.

2.2. Methods

The microstructure of the NAFP glass was investigated by scanning electron microscopy (SEM) using a Mira3 microscope (Tescan, Brno, Czech Republic), and electron probe microanalysis of the samples was conducted by energy-dispersive X-ray spectroscopy (EDS) using an analyzer X-Max (Oxford Inst., High Wycombe, UK).

The thermal stability of the samples containing the spent electrolyte imitation and zeolite was studied in accordance with the current requirements [23] for solidified HLW. This treatment includes heating to 450 °C for 4 h as an available simulation of thermal heating of materials, occurring due to the radioactive decay of HLW radionuclides [9]. The samples of the MPP-Z compound were preliminarily kept at 180 °C for 10 h for removal of bound water from MgKPO₄·6H₂O-based compounds in a muffle furnace SNOL 30/1300 (AB UMEGA GROUP, Utena, Lithuania), as previously shown in [11].

The hydrolytic stability of the obtained samples was determined in accordance with the semi-dynamic standard GOST R 52126-2003 at 25 ± 3 °C [24]. In accordance with the standard, monolithic samples with known open geometric surface area were placed in distilled water used as a leaching agent, as well as solutions of hydrogen peroxide H₂O₂ (TU 2123-002-25665344-2008, Rushim LLC, Moscow, Russia) as a imitation of groundwater radiolysis products. The pH of the leaching solutions was 6.6 ± 0.1 for distilled water, and 4.0 ± 0.1 and 3.5 ± 0.1 for 0.7 wt.% and 7.0 wt.% H₂O₂ solution, respectively. The content of hydrogen peroxide was calculated on the basis of a number of assumptions; the energy release of HLW was 3.0 kJ/(s·t) [12]; the radiation chemical yield of hydrogen peroxide during radiolysis of water was 0.075 μmol/J [12]; the working volume of the container with solidified HLW was 0.2 m³; the limiting volume of the contact solution, which could be near the container with solidified HLW, was taken equal to the ratio of the volume of the contact solution to the area of open geometric surface of the sample (V/S) 3–10 times; the radiation energy was completely absorbed by the contact solution and led to the formation of H₂O₂ [12]. Taking these assumptions into account, the maximum content of hydrogen peroxide in contact aqueous solution after 10 and 100 years was calculated, and the result was equal to 0.7 wt.% and 7.0 wt.% H₂O₂, respectively. Leaching of samples of NAFP glass and MPP compound was carried out at a V/S ratio of 3 and 7, respectively. Before leaching, samples of the compound were immersed in ethanol for 5–7 s, and then the samples were

air-dried for 30 min. The leaching agent was periodically replaced after 1, 3, 7, 10, 14, 21, and 28 days. Leaching was carried out in a tightly closed PTFE container. The leached solution was decanted and acidified to pH 1, and the new portion of leaching agent was poured onto the samples. The pH measurement after leaching was measured on a pH meter (Expert-pH, Econiks-Expert LLC, Moscow, Russia). The pH measurement error of three parallel solutions was no more than 2% in solutions after leaching of the MPP compound and no more than 5% in solutions after leaching of the NAFF glass. The content of the components in the solution after leaching was determined by ICP-AES (iCAP-6500 Duo, Thermo Scientific, Waltham, MA, USA) and ICP-MS (X Series2, Thermo Scientific, Waltham, MA, USA). The experimental and instrumental errors did not exceed the relative values of 30% due to the low contents of elements in solutions after leaching.

The differential leaching rate LR ($\text{g}/(\text{cm}^2 \cdot \text{day})$) of the components was calculated as follows:

$$\text{LR} = \frac{c \cdot V}{S \cdot f \cdot t},$$

where c is the element concentration in solution after leaching (g/L), V is the volume of leaching agent (L), S is the sample surface (cm^2), f is the element content in the matrix (g/g), t is the duration of the n -th leaching period between replacements of contact solution (days).

3. Results and Discussion

3.1. Study of NAFF Glass after Contact with Hydrogen Peroxide

3.1.1. Hydrolytic Stability of Samples

The results of the leaching of sodium and phosphorus, as the main structure-forming components, from the studied samples of NAFF glass in solutions of 0.7 wt.% and 7.0 wt.% H_2O_2 , are presented in Figures 1 and 2, respectively. In addition, the results of leaching of sodium and phosphorus from glass in a solution of distilled water are also presented in Figures 1 and 2 for comparison. It was noted that the leaching of sodium was similar to the leaching of phosphorus, and their differential leaching rate from glass samples increased during leaching in H_2O_2 solutions (Figure 1). The differential leaching rate of sodium from the heat-treated samples (Figure 1b) approximately corresponded to the leaching rate of Na from the original samples (Figure 1a), and it was approximately $2.0 \times 10^{-6} \text{ g}/(\text{cm}^2 \cdot \text{day})$ on the 28th day upon contact with distilled water, whereas, after contact with 0.7 wt.% and 7.0 wt.% H_2O_2 solutions, leaching rates of Na were $3.6\text{--}9.6 \times 10^{-6}$ and $2.6\text{--}3.8 \times 10^{-5} \text{ g}/(\text{cm}^2 \cdot \text{day})$, respectively. It should be noted that the sodium leaching rate is not a normalized criterion for the quality of the compound; however, due to the similarity of the chemical behavior of ions of Na and Cs, with a certain degree of approximation, we can focus on the requirements for the ^{137}Cs leaching rate. Thus, the leaching rate of ^{137}Cs from a glassy compound at 25°C should not exceed $10^{-5} \text{ g}/(\text{cm}^2 \cdot \text{day})$ [23]. This condition was observed on the 28th day of contact with distilled water and in the case of 0.7 wt.% H_2O_2 for both the initial and the heat-treated samples. The same order of magnitude of leaching rate of the sodium was observed for base glass without the addition of waste simulants [25]. The differential leaching rate of phosphorus from the samples on the 28th day of their contact with distilled water was $5.5\text{--}8.5 \times 10^{-7} \text{ g}/(\text{cm}^2 \cdot \text{day})$, whereas, after contact with the solutions of 0.7 wt.% and 7.0 wt.% H_2O_2 , these rates were $(0.1\text{--}7.2) \times 10^{-6} \text{ g}/(\text{cm}^2 \cdot \text{day})$ and about $8.8 \times 10^{-5} \text{ g}/(\text{cm}^2 \cdot \text{day})$, respectively (Figure 2). The concentration of components of the spent electrolyte imitation in solutions after leaching of NAFF glass was below the detection limits of the ICP-AES method.

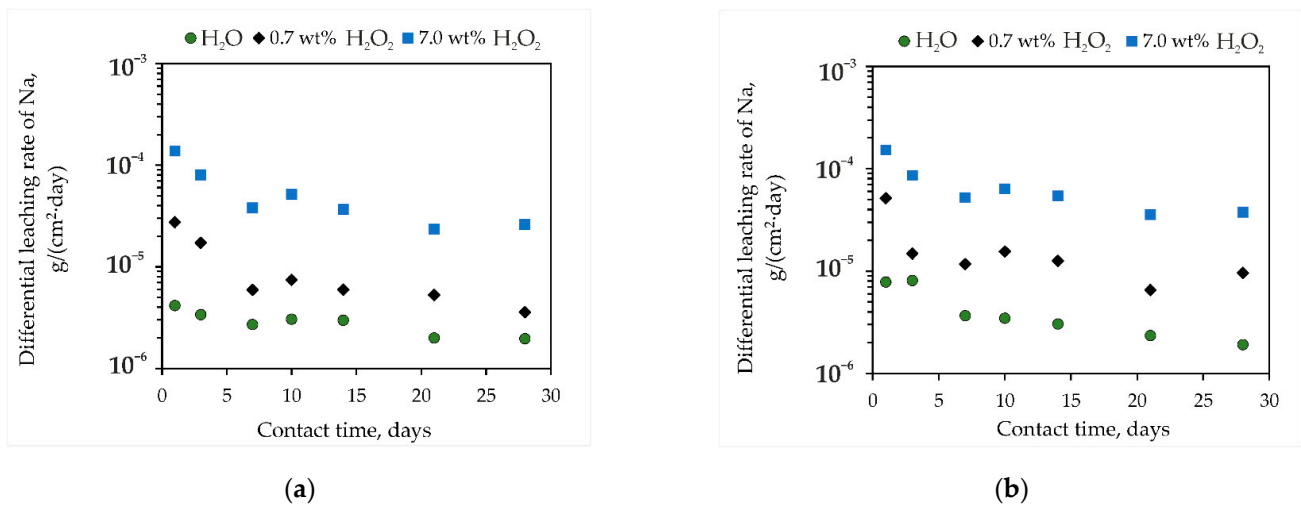


Figure 1. Kinetic curves of the leaching rate of Na from (a) initial samples of NAFP glass and (b) samples after heat treatment at 450 °C.

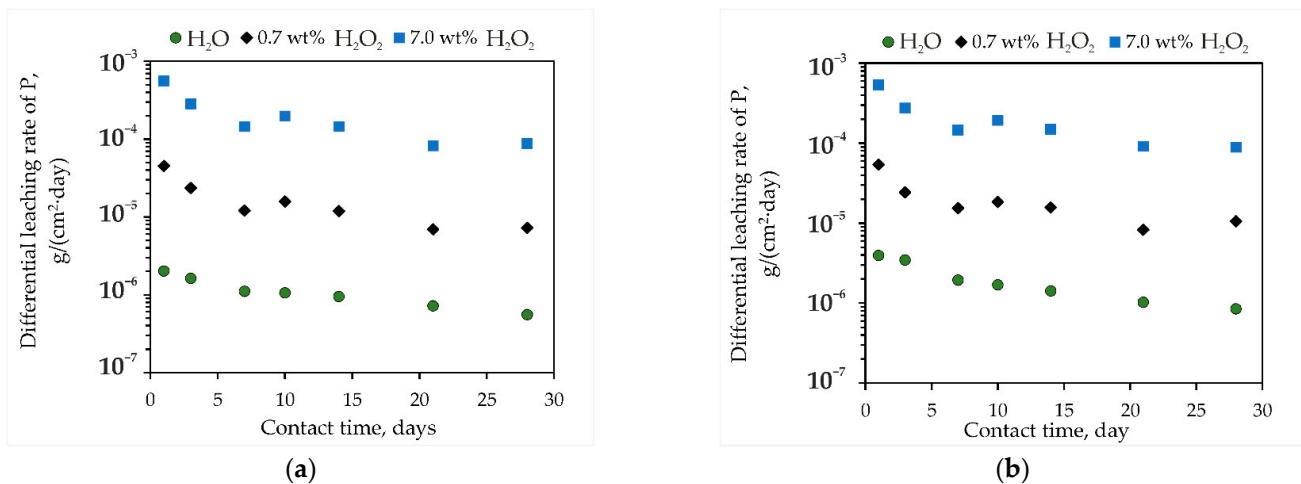


Figure 2. Kinetic curves of the leaching rate of P from (a) initial samples of NAFP glass and (b) samples after heat treatment at 450 °C.

Figure 3 shows the results of measuring the pH of solutions after leaching the glass samples. It is shown that the pH of the samples after leaching in distilled water resided in the alkaline region, whereas that after leaching in H₂O₂ solutions resided in the acidic region. It was established that the leaching of glass components did not lead to a change in the pH of the solution at a high concentration of hydrogen peroxide (7.0 wt.%) in the contact solution, and the pH remained stable within 3.5 ± 0.5 , except for solutions after leaching of heat-treated glass samples after the first day of contact. This was probably due to the greater leaching from the sample surface because of the surface layer formed on it, as noted in [9]. For a 0.7 wt.% hydrogen peroxide solution, the pH was 4.5–6.0. In [12,16], the authors noted that the main mechanisms of leaching of glass elements, such as ion exchange and hydrolysis, were quite dependent on the pH of the solution. The leaching rate of ion exchange decreases with increasing pH, while the rate of hydrolysis, on the contrary, increases. During radiolysis, the amount of H₃O⁺ ions in the contact solution gradually increases, such that the pH remains at a level close to neutral. These ions penetrate deep into the surface layer through ion exchange, neutralize the hydroxide ions formed in the modified surface layer, and prevent hydrolytic dissolution of the glass frame, increasing its chemical stability. Thus, in this study, a positive effect of the presence of H₂O₂ in the contact solution was noted. However, in [17], the authors noted a decrease in pH by 1 already at a concentration of 1.51×10^{-5} mol/L H₂O₂ that resulted in a negative effect on the

leaching rate of glass components, which became especially noticeable after 20 days of leaching. In our case, we also observed a negative effect of the presence of H_2O_2 in the contact solution and a decrease in leaching rate, and this effect was typical from the first day of the experiment.

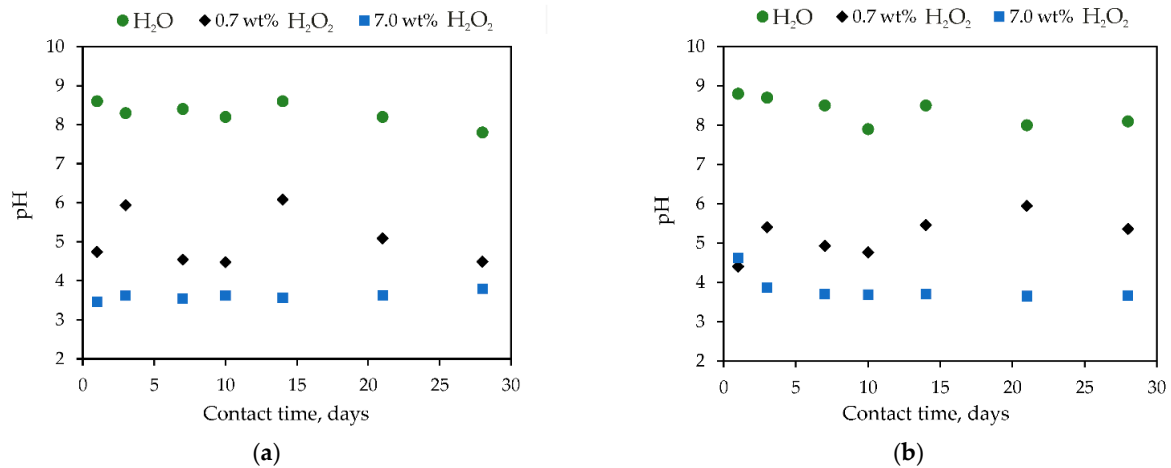


Figure 3. The pH values of solutions after leaching (a) initial samples of NAFF glass and (b) samples after heat treatment at $450\text{ }^\circ\text{C}$.

3.1.2. Surface of Samples

SEM images of NAFF glass samples after their contact with 0.7 wt.% hydrogen peroxide solution, including after their heat treatment at $450\text{ }^\circ\text{C}$, are shown in Figure 4, and the data on the elemental composition of the studied samples are presented in Table 2. It can be noted that the initial samples consisted of two phases (Figure 4a). Hence, the formation of a separate phase (Phase #2, Figure 4a, Table 2), probably mixed sodium–iron–aluminum pyrophosphates on the surface of the glass phase, occurred (Phase #1, Figure 4a, Table 2). After contact of samples which were previously heat-treated at $450\text{ }^\circ\text{C}$ with a hydrogen peroxide solution, the thickness of the surface layer increased (Figure 4c) and was about $10\text{ }\mu\text{m}$ (the initial thickness was $2\text{--}3\text{ }\mu\text{m}$ and was represented mainly by a mixture of sodium–iron–aluminum pyrophosphates, as well as a phase containing sodium and chlorine [7]).

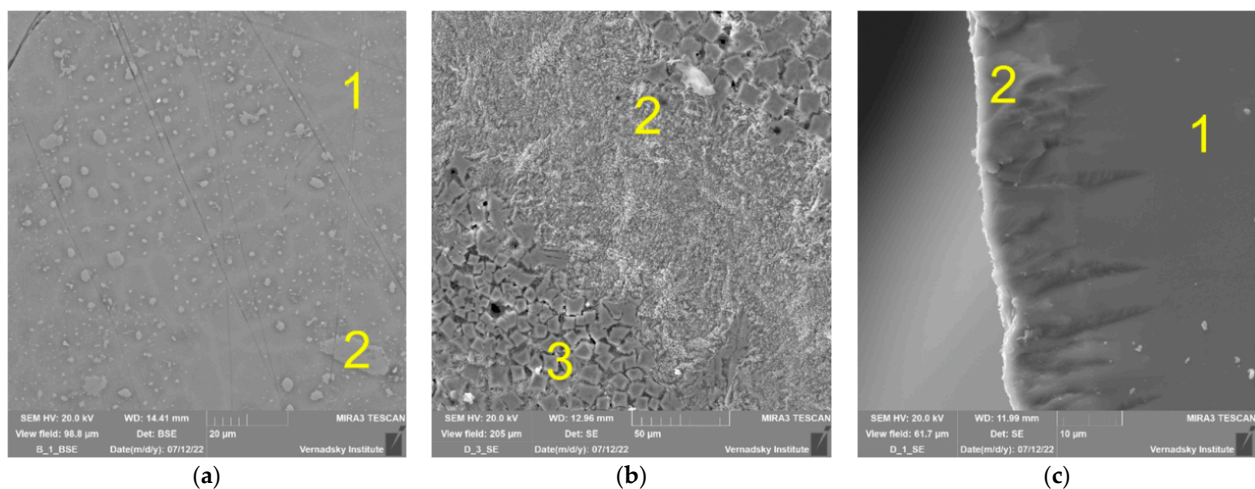


Figure 4. SEM images of NAFF glass after leaching in a 0.7 wt.% H_2O_2 solution: (a) the surface of the initial sample; (b) the surface of the sample after heat treatment at $450\text{ }^\circ\text{C}$; (c) the surface layer boundary of the heat-treated glass.

Table 2. The semiquantitative elemental composition (wt.%) of samples of NAFF glass after contact with a 0.7 wt.% H₂O₂ solution.

Element	Phase #1	Phase #2	Phase #3
Na	14.1 ± 2.1	12.0 ± 1.8	10.5 ± 1.6
P	21.5 ± 3.2	20.7 ± 3.1	22.3 ± 3.3
Fe	10.6 ± 1.6	12.9 ± 1.9	22.1 ± 3.3
Al	4.7 ± 0.7	4.8 ± 0.7	3.1 ± 0.5
K	1.8 ± 0.3	1.8 ± 0.3	-
Cs	0.1 ± 0.1	0.1 ± 0.1	-
La	2.4 ± 0.4	2.3 ± 0.4	-
Sr	0.2 ± 0.1	0.1 ± 0.1	-
Ba	0.3 ± 0.1	0.4 ± 0.1	-
Cl	0.9 ± 0.2	1.1 ± 0.2	-
O	42.3 ± 6.3	42.8 ± 6.4	41.8 ± 6.3
Si	1.1 ± 0.2	1.0 ± 0.2	0.2 ± 0.1

Moreover, in-depth dendritic formations of crystalline phases formed in the glass phase (Figure 4c). The resulting phase was close in composition to the original glass composition and probably consisted of mixed sodium–iron–aluminum pyrophosphates (Phase #2, Figure 4a, Table 2). There were two phases on the surface (Figure 4b): a sample-covering mixed pyrophosphate phase (Phase #2, Figure 4b, Table 2), and a pyrophosphate phase with predominant isolation of cubic iron pyrophosphate (Phase #3, Figure 4b, Table 2). It should be noted that the content of chlorine in all detected phases of the samples was low, and the sodium chloride phase (Phase #3, Figure 4b, Table 2) found in the heat-treated samples before contact with the H₂O₂ solution was absent [7], which may indicate its dissolution during the leaching process.

SEM images of NAFF glass samples after their contact with hydrogen peroxide at a concentration of 7.0 wt.%, including after their heat treatment at 450 °C, are shown in Figure 5, and the data on the elemental composition of the studied samples are presented in Table 3. It was found that the surface of the original glass samples was inhomogeneous and consisted of three phases (Figure 5a) with small pores up to 50 µm. The main glass phase was represented by an uneven surface with micropores (Phase #1, Figure 5c, Table 3), and the formed phase, as in the case of leaching in a 0.7 wt.% H₂O₂ solution, was represented by mixed pyrophosphates with the predominant formation of iron pyrophosphate (Phase #2, Figure 5a, Table 3). In addition, the formation of elongated crystals of the aluminum oxide phase was observed in a small amount (Phase #3, Figure 5a, Table 3). After contact of glass samples which were previously heat-treated at 450 °C with a hydrogen peroxide solution, a surface layer with a thickness of almost 10 µm also consisted of a pyrophosphate phase with a predominance of iron pyrophosphate, uniformly covering the entire surface of the sample (Phase #2, Figure 5b,c, Table 3).

Thus, after the contact of the initial samples with H₂O₂ solutions, new phases formed on their surface. Most of the surface of the sample was represented by the original glass phase, and the crystalline phases had a focal characteristic. After leaching of heat-treated samples, the thickness of the surface layer increased. However, as can be seen from the leaching results (Figures 1 and 2), the contact solution had a greater effect on the leaching rate than heat treatment and, accordingly, the process of the formation of a surface crystalline layer.

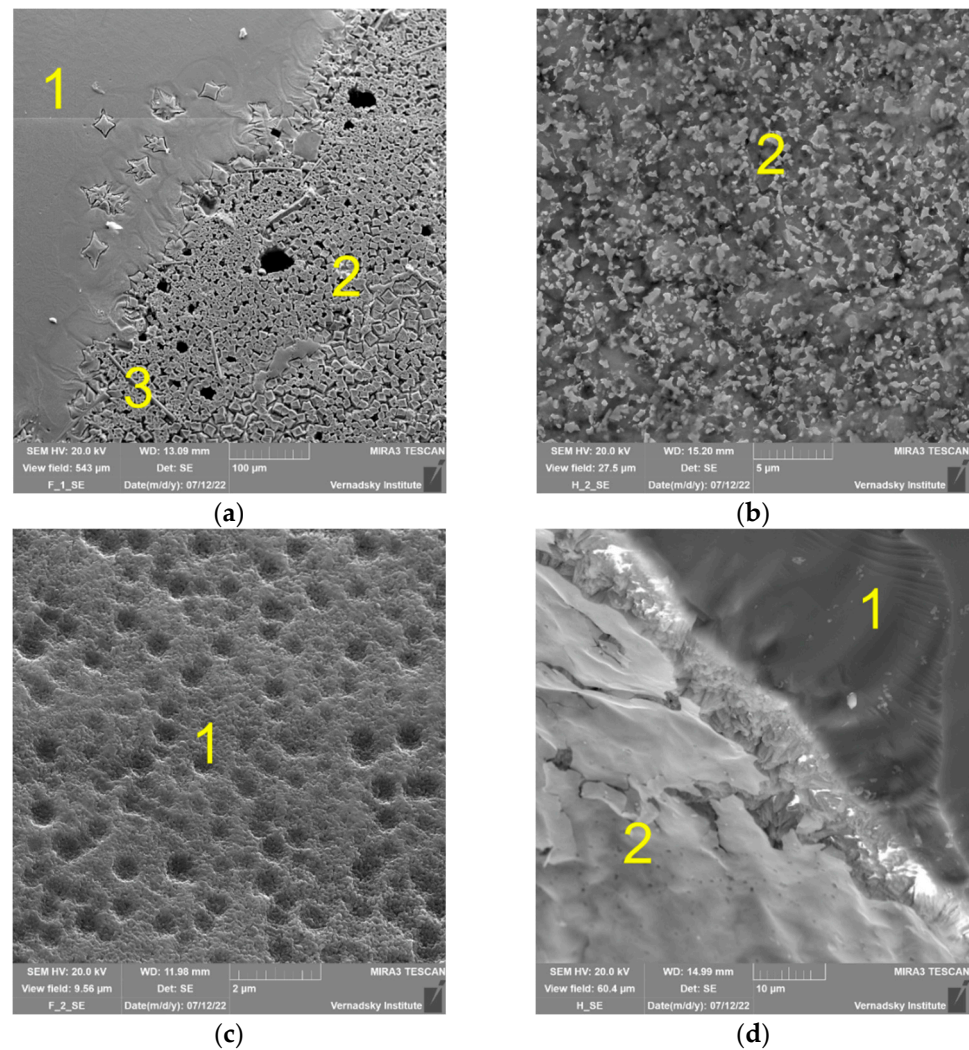


Figure 5. SEM images of NAFP glass after leaching in a 7.0 wt.% H_2O_2 solution: (a,b) the surface of the initial sample; (c) the surface of the sample after heat treatment at 450 °C; (d) the surface layer boundary of the heat-treated glass.

Table 3. The semiquantitative elemental composition (wt.%) of samples of NAFP glass after contact with a 7.0 wt.% H_2O_2 solution.

Element	Phase #1	Phase #2	Phase #3
Na	14.1 ± 2.1	12.1 ± 1.8	1.2 ± 0.2
P	21.2 ± 3.2	22.2 ± 3.3	8.5 ± 1.3
Fe	9.8 ± 1.5	20.6 ± 3.1	7.2 ± 1.1
Al	5.2 ± 0.8	3.1 ± 0.5	34.7 ± 5.2
K	1.5 ± 0.2	-	0.5 ± 0.1
Cs	0.1 ± 0.1	-	-
La	1.9 ± 0.3	-	2.2 ± 0.3
Sr	0.2 ± 0.1	-	-
Ba	0.3 ± 0.1	-	-
Cl	1.4 ± 0.2	-	0.2 ± 0.1
O	42.8 ± 6.4	41.8 ± 6.3	45.1 ± 6.8
Si	1.5 ± 0.2	0.2 ± 0.1	0.4 ± 0.1

3.2. Study of MPP-Z Compound after Contact with Hydrogen Peroxide

The obtained data on the differential leaching rate of compound components from MPP-Z compound samples after its heat treatment at 180 °C and 450 °C in 0.7 wt.%

and 7.0 wt.% H_2O_2 solutions, including in distilled water for comparison, are shown in Figures 6 and 7, respectively. It was found that the content of hydrogen peroxide in the contact solution had almost no effect on the resistance of the compound to potassium leaching (Figures 6c and 7c), but led to a significant increase in the leaching rate of magnesium and phosphorus (Figures 6a, 7a, 6b and 7b, respectively). Thus, the differential leaching rate of magnesium from the MPP-Z compound regarding the results of contact in distilled water increases up to fourfold and by an order of magnitude at the content of hydrogen peroxide in 0.7 and 7.0 wt.% H_2O_2 solutions, respectively. In this case, the leaching rate of magnesium in H_2O_2 solutions was $0.5\text{--}1.4 \times 10^{-3} \text{ g}/(\text{cm}^2 \cdot \text{day})$, whereas those of phosphorus and potassium were $0.7\text{--}1.5 \times 10^{-3}$ and about $5.7 \times 10^{-4} \text{ g}/(\text{cm}^2 \cdot \text{day})$, respectively. It was noted that the leaching rate of matrix-forming components from MPP-Z compound samples after its heat treatment at $450 \text{ }^\circ\text{C}$ was the same as from MPP-Z compound samples after its heat treatment at $180 \text{ }^\circ\text{C}$. Using the example of strontium leaching from MPP-Z compound samples, it was shown that the differential leaching rate of strontium (Figures 6d and 7d) increased with an increase in the content of hydrogen peroxide in leaching solutions by up to two orders of magnitude and did not depend on the heat treatment of the compound. Thus, the differential leaching rate of strontium from MPP-Z compound samples was $5.0\text{--}6.3 \times 10^{-4} \text{ g}/(\text{cm}^2 \cdot \text{day})$ in a concentrated H_2O_2 solution, lower than the regulatory requirements for solidified HLW [23]. The values of pH of the solutions after leaching did not vary much in both cases of temperatures of $180 \text{ }^\circ\text{C}$ and $450 \text{ }^\circ\text{C}$, residing in a neutral–alkaline area (7.5–9.3) depending on the time of solution change (Figure 8).

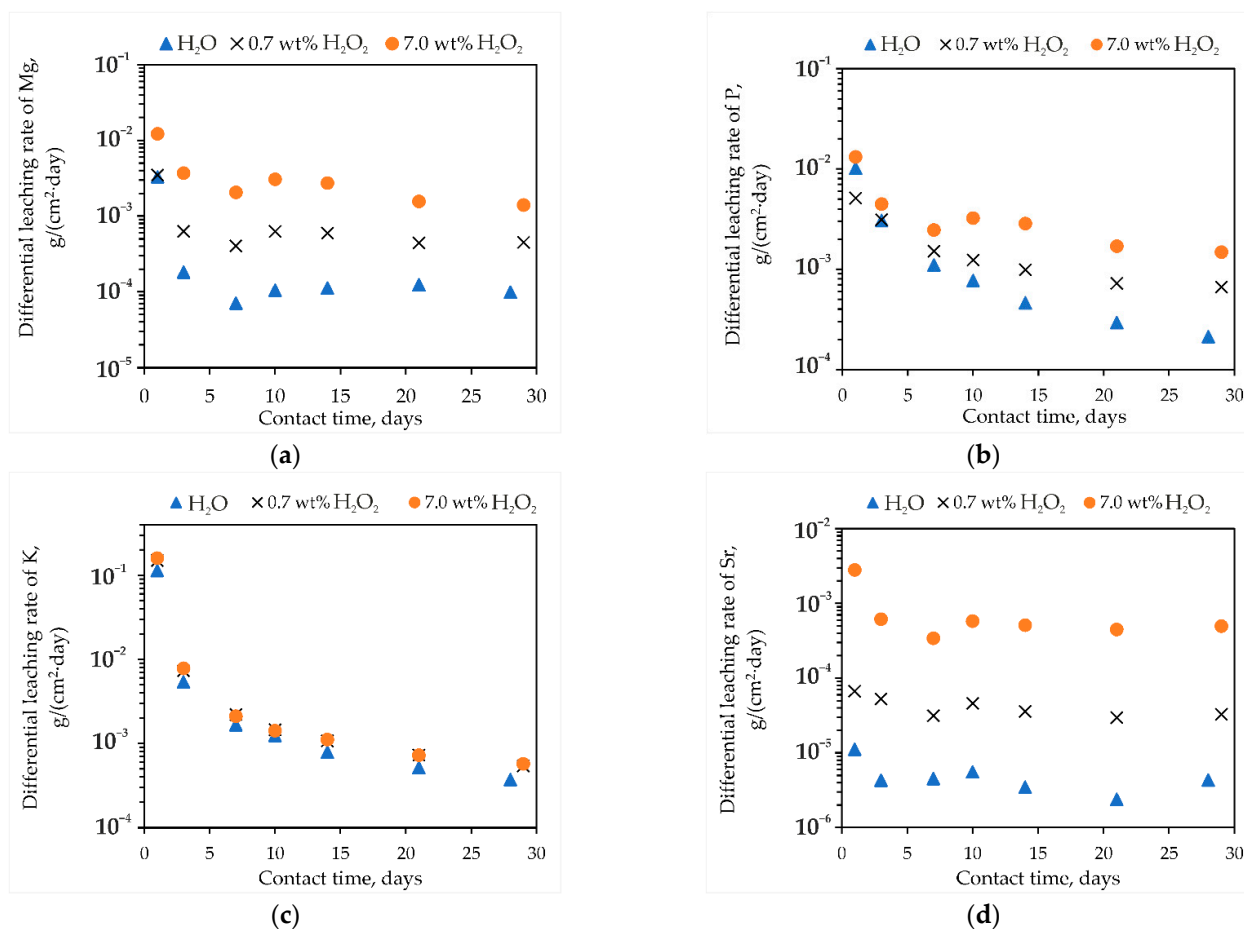


Figure 6. Kinetic curves of the leaching rates of (a) Mg, (b) P, (c) K, and (d) Sr from MPP-Z compound after its heat treatment at $180 \text{ }^\circ\text{C}$ as a function of the hydrogen peroxide content in the contact solution.

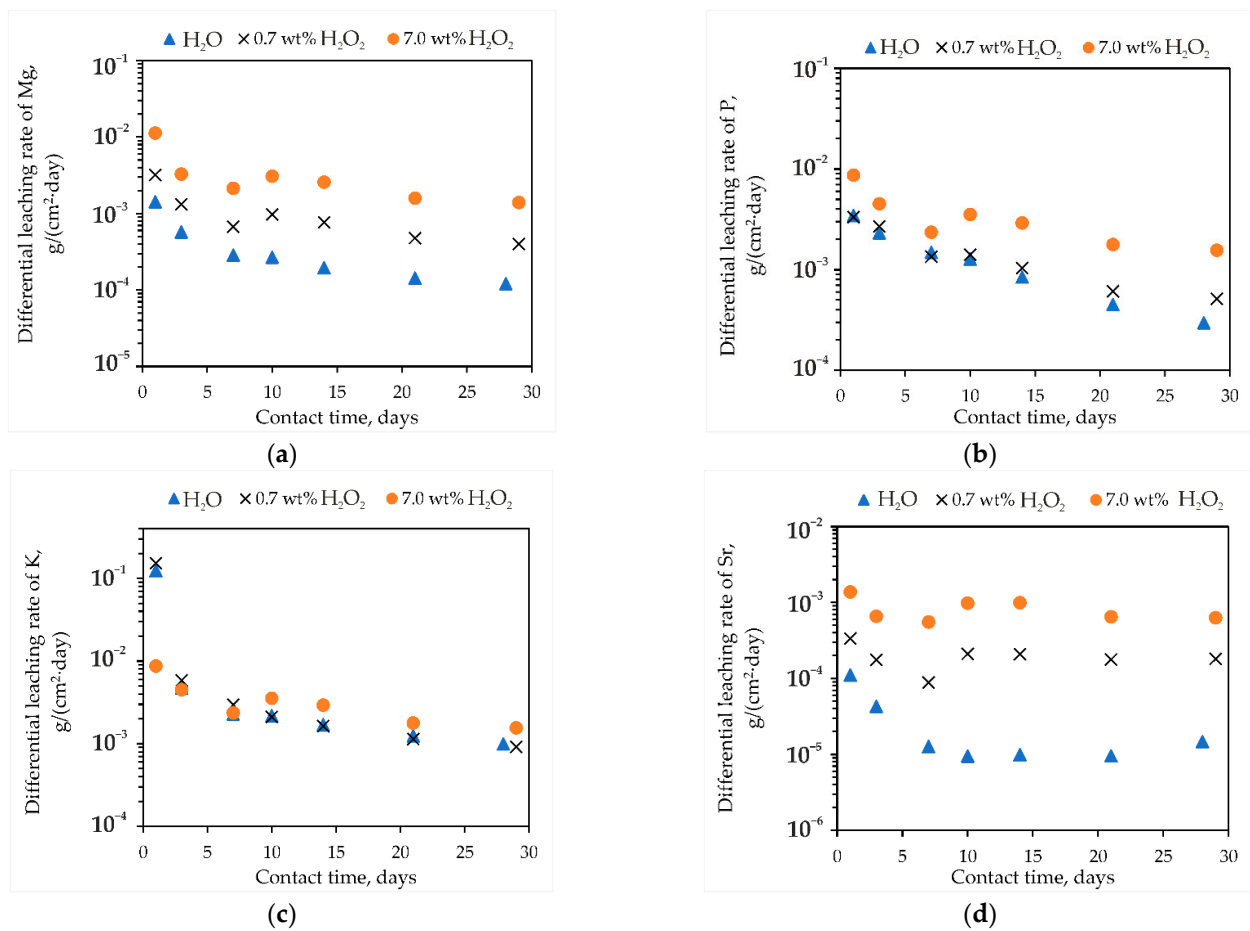


Figure 7. Kinetic curves of the leaching rates of (a) Mg, (b) P, (c) K, and (d) Sr from MPP-Z compound after its heat treatment at 450 °C as a function of the hydrogen peroxide content in the contact solution.

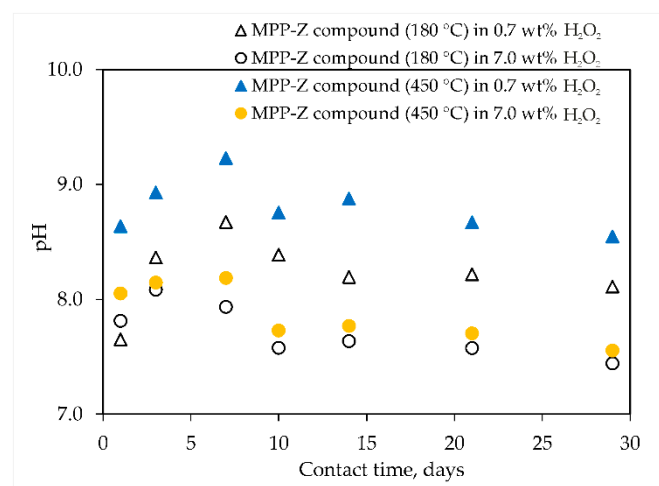


Figure 8. The pH values of solutions after leaching of samples of MPP-Z compounds in hydrogen peroxide solutions.

It can be noted that, after keeping the MPP-Z compound samples for 28 days in hydrogen peroxide solutions, the surface of the studied samples changed significantly (Figures 9 and 10), which was the cause of the increase in compound component leaching. Thus, the negative effect of the accumulation of hydrogen peroxide in natural water as a product of its radiolysis on the hydrolytic stability of the compound should be taken into account when justifying the radiation safety of solidified HLW disposal.

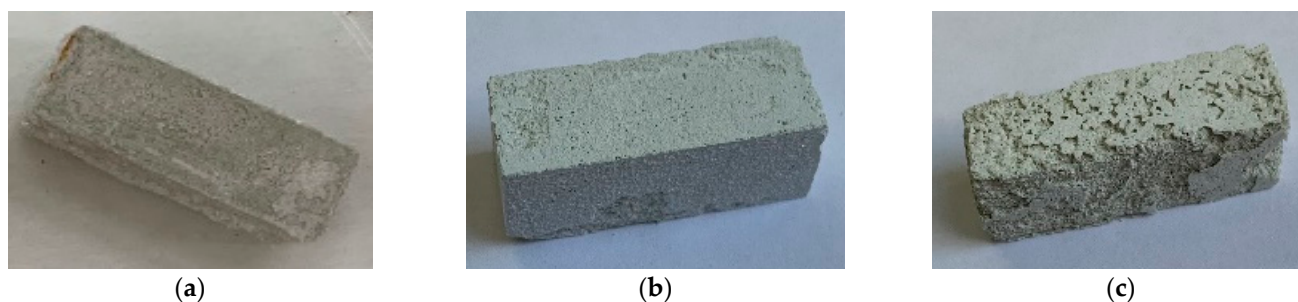


Figure 9. Photos (a) of the MPP-Z compound after its heat treatment at 180 °C, including after soaking in solutions of (b) 0.7 wt.% and (c) 7.0 wt.% hydrogen peroxide.

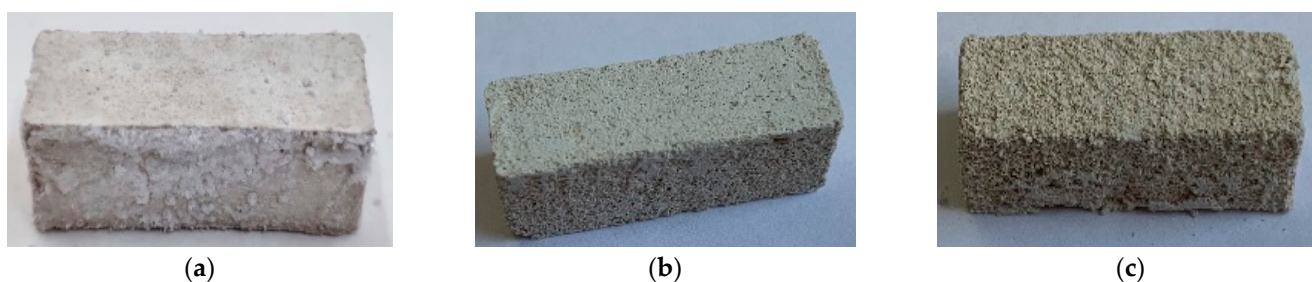


Figure 10. Photos (a) of the MPP-Z compound after its heat treatment at 450 °C, including after soaking in solutions of (b) 0.7 wt.% and (c) 7.0 wt.% hydrogen peroxide.

4. Conclusions

It was shown that NAFP glass and MPP-Z compounds with an immobilized spent electrolyte imitation had a high hydrolytic stability. Samples of NAFP glass after leaching in hydrogen peroxide solutions were prone to the precipitation of crystalline phases on the surface, represented mainly by a mixture of sodium–iron–aluminum pyrophosphates. It was found that an increase in the content of hydrogen peroxide in the contact water as a product of its radiolysis led to a decrease in the hydrolytic stability of the compounds after contact with this aqueous solution. Thus, the leaching rate of sodium and phosphorus was increased up to eight- and 100-fold during contact of the NAFP compound with 0.7 and 7.0 wt.% hydrogen peroxide solutions, respectively. When placing the MPP-Z compound in natural water containing up to 0.7 and 7.0 wt.% hydrogen peroxide for simulating of radiolysis process, it was shown that the leaching rate of potassium did not change; however, for magnesium, phosphorus, and strontium, it increased by about four- and up to 100-fold for 0.7 and 7.0 wt.% hydrogen peroxide, respectively. The increased leaching was confirmed by the change in the surface of the samples. Therefore, the detected negative factors of the presence of radiolytic hydrogen peroxide in natural water should be taken into account when choosing matrices for spent electrolyte immobilization. Thus, the results obtained should be used to justify the radiation safety of the conditioning and disposal of such waste.

Author Contributions: Conceptualization, S.A.K., A.V.F. and S.S.D.; methodology, A.V.F., S.A.K., S.S.D. and S.E.V.; validation, A.V.F. and S.A.K.; formal analysis, A.V.F., S.A.K., S.S.D. and K.Y.B.; investigation, A.V.F. and K.Y.B.; resources, S.E.V.; writing—original draft preparation, A.V.F. and S.A.K.; writing—review and editing, S.E.V.; visualization, S.A.K. and S.E.V.; supervision, S.E.V.; project administration, S.E.V.; funding acquisition, S.E.V. All authors have read and agreed to the published version of the manuscript.

Funding: The work was supported by the Ministry of Science and Higher Education of Russia (grant agreement No. 075-15-2020-782).

Institutional Review Board Statement: Not applicable.

Informed Consent Statement: Not applicable.

Data Availability Statement: Not applicable.

Acknowledgments: The authors thank I.N. Gromyak and A.V. Zhilkina (Laboratory of Methods for Investigation and Analysis of Substances and Materials, GEOKHI RAS) for performing the ICP-AES and ICP-MS analysis, as well as S.I. Demidova (Meteoritics laboratory, GEOKHI RAS) for the analysis of samples using SEM-EDS.

Conflicts of Interest: The authors declare no conflict of interest. The funders had no role in the design of the study; in the collection, analyses, or interpretation of data; in the writing of the manuscript, or in the decision to publish the results.

References

1. Ma, B.; Charlet, L.; Fernandez-Martinez, A.; Kang, M.; Made, B. A review of the retention mechanisms of redox-sensitive radionuclides in multi-barrier systems. *Appl. Geochem.* **2019**, *100*, 414–431. [[CrossRef](#)]
2. Donald, I.W. *Waste Immobilization in Glass and Ceramic Based Hosts: Radioactive, Toxic and Hazardous Wastes*; John Wiley & Sons: West Sussex, UK, 2010; pp. 1–507, ISBN 978-1-4443-1937-8.
3. Ojovan, M.I.; Petrov, V.A.; Yudin, S.V. Glass Crystalline Materials as Advanced Nuclear Wasteforms. *Sustainability* **2021**, *13*, 4117. [[CrossRef](#)]
4. McCloy, J.S.; Schuller, S. Vitrification of wastes: From unwanted to controlled crystallization, a review. *Comptes Rendus Géosci.* **2022**, *354*, 1–40, *online first*. [[CrossRef](#)]
5. Poluektov, P.P.; Schmidt, O.V.; Kascheev, V.A.; Ojovan, M.I. Modelling aqueous corrosion of nuclear waste phosphate glass. *J. Nucl. Mater.* **2017**, *484*, 357–366. [[CrossRef](#)]
6. Choi, J.; Um, W.; Choung, S. Development of iron phosphate ceramic waste form to immobilize radioactive waste solution. *J. Nucl. Mater.* **2014**, *452*, 16–23. [[CrossRef](#)]
7. Shadrin, A.Y.; Dvoeglazov, K.N.; Maslennikov, A.G.; Kashcheev, V.A.; Tret'yakova, S.G.; Shmidt, O.V.; Vidanov, V.L.; Ustinov, O.A.; Volk, V.I.; Veselov, S.N.; et al. PH process as a technology for reprocessing mixed uranium-plutonium fuel from BREST-OD-300 reactor. *Radiochemistry* **2016**, *58*, 271–279. [[CrossRef](#)]
8. Donald, I.W.; Metcalfe, B.L.; Fong, S.K.; Gerrard, L.A.; Strachan, D.M.; Scheele, R.D. A glass-encapsulated calcium phosphate wasteform for the immobilization of actinide-, fluoride-, and chloride-containing radioactive wastes from the pyrochemical reprocessing of plutonium metal. *J. Nucl. Mater.* **2007**, *361*, 78–93. [[CrossRef](#)]
9. Kulikova, S.A.; Danilov, S.S.; Matveenko, A.V.; Frolova, A.V.; Belova, K.Y.; Petrov, V.G.; Vinokurov, S.E.; Myasoedov, B.F. Perspective Compounds for Immobilization of Spent Electrolyte from Pyrochemical Processing of Spent Nuclear Fuel. *Appl. Sci.* **2021**, *11*, 1180. [[CrossRef](#)]
10. Danilov, S.S.; Frolova, A.V.; Kulikova, S.A.; Vinokurov, S.E.; Maslakov, K.I.; Teterin, A.Y.; Teterin, Y.A.; Myasoedov, B.F. Immobilization of Rhenium as a Technetium Surrogate in Aluminum Iron Phosphate Glass. *Radiochemistry* **2021**, *63*, 99–106. [[CrossRef](#)]
11. Kulikova, S.A.; Belova, K.Y.; Tyupina, E.A.; Vinokurov, S.E. Conditioning of Spent Electro-lyte Surrogate LiCl-KCl-CsCl Using Magnesium Potassium Phosphate Compound. *Energies* **2020**, *13*, 1963. [[CrossRef](#)]
12. Aloy, A.S.; Nikandrova, M.V. Leaching of borosilicate glasses containing simulated high-level waste in solutions of hydrogen peroxide as a substance simulating radiolysis products. *Radiochemistry* **2014**, *56*, 633–638. [[CrossRef](#)]
13. McVay, G.L.; Pederson, L.R. Effect of gamma radiation on glass leaching. *J. Am. Ceram. Soc.* **1981**, *64*, 154–158. [[CrossRef](#)]
14. Barkatt, A.; Barkatt, A.; Sousanpour, W. Gamma radiolysis of aqueous media and its effects on the leaching processes of nuclear waste disposal materials. *Nucl. Technol.* **1983**, *60*, 218–227. [[CrossRef](#)]
15. Rolland, S.; Tribet, M.; Jollivet, P.; Jegou, C.; Broudic, V.; Marques, C.; Ooms, H.; Toulhoat, P. Influence of gamma irradiation effects on the residual alteration rate of the French SON68 nuclear glass. *J. Nucl. Mater.* **2013**, *433*, 382–389. [[CrossRef](#)]
16. Ojovan, M.I.; Lee, W.E. Glassy wasteforms for nuclear waste immobilisation. *Metall. Mater. Trans. A* **2011**, *42*, 837–851. [[CrossRef](#)]
17. Abdelouas, A.; Ferrand, K.; Grambow, B.; Mennecart, T.; Fattahi, M.; Blondiaux, G.; Houee-Levin, C. Effect of gamma and alpha irradiation on the corrosion of the French borosilicate glass SON 68. *MRS Online Proc. Libr.* **2003**, *807*, 397–402. [[CrossRef](#)]
18. Vance, E.R.; Davis, J.; Olufson, K.; Chironi, I.; Karatchevtseva, I.; Farnan, I. Candidate waste forms for immobilisation of waste chloride salt from pyroprocessing of spent nuclear fuel. *J. Nucl. Mater.* **2012**, *420*, 396–404. [[CrossRef](#)]
19. Stefanovsky, S.V.; Stefanovskaya, O.I.; Vinokurov, S.E.; Danilov, S.S.; Myasoedov, B.F. Phase composition, structure, and hydrolytic durability of glasses in the Na₂O-Al₂O₃-(Fe₂O₃)-P₂O₅ system at replacement of Al₂O₃ by Fe₂O₃. *Radiochemistry* **2015**, *57*, 348–355. [[CrossRef](#)]
20. Stefanovskii, S.V.; Stefanovskaya, O.I.; Semenova, D.V.; Kadyko, M.I.; Danilov, S.S. Phase Composition, Structure, and Hydrolytic Stability of Sodium-Aluminum(Iron) Phosphate Glass Containing Rare-Earth Oxides. *Glas. Ceram.* **2018**, *75*, 89–94. [[CrossRef](#)]
21. Maslakov, K.I.; Teterin, Y.A.; Stefanovsky, S.V.; Kalmykov, S.N.; Teterin, A.Y.; Ivanov, K.E.; Danilov, S.S. XPS study of neptunium and plutonium doped iron-bearing and iron-free sodium-aluminum-phosphate glasses. *J. Non-Cryst. Solids* **2018**, *482*, 23–29. [[CrossRef](#)]

22. Kulikova, S.A.; Vinokurov, S.E. The Influence of Zeolite (Sokyrnytsya Deposit) on the Physical and Chemical Resistance of a Magnesium Potassium Phosphate Compound for the Immobilization of High-Level Waste. *Molecules* **2019**, *24*, 3421. [[CrossRef](#)] [[PubMed](#)]
23. NP-019-15; Federal Norms and Rules in the Field of Atomic Energy Use “Collection, Processing, Storage and Conditioning of Liquid Radioactive Waste. Safety Requirements”. With Changes (Order No. 299 Dated 13.09.2021). Rostekhnadzor: Moscow, Russia, 2015; pp. 1–22.
24. GOST R 52126-2003; Radioactive Waste. Long Time Leach Testing of Solidified Radioactive Waste Forms. Gosstandart 305: Moscow, Russia, 2003; pp. 1–8.
25. Danilov, S.S.; Kulikova, S.A.; Frolova, A.V.; Vinokurov, S.S. Sodium alumino-iron phosphate glass application for immobilizing technetium containing waste. In Proceedings of the ChemCys 2020, Blankenberge, Belgium, 19–21 February 2020.